The American Journal of Pathology, Vol. 180, No. 6, June 2012

http://dx.doi.org/10.1016/j.ajpath.2012.02.019

Vascular Biology, Atherosclerosis, and Endothelium Biology

Plasticity of Button-Like Junctions in the Endothelium of Airway Lymphatics in Development and Inflammation

Li-Chin Yao,* Peter Baluk,*
R. Sathish Srinivasan,† Guillermo Oliver,†
and Donald M. McDonald*

From the Department of Anatomy, Cardiovascular Research Institute, and the Comprehensive Cancer Center, University of California, San Francisco, California; and the Department of Genetics and Tumor Cell Biology,† St Jude Children's Research Hospital, Memphis, Tennessee*

Endothelial cells of initial lymphatics have discontinuous button-like junctions (buttons), unlike continuous zipper-like junctions (zippers) of collecting lymphatics and blood vessels. Buttons are thought to act as primary valves for fluid and cell entry into lymphatics. To learn when and how buttons form during development and whether they change in disease, we examined the appearance of buttons in mouse embryos and their plasticity in sustained inflammation. We found that endothelial cells of lymph sacs at embryonic day (E)12.5 and tracheal lymphatics at E16.5 were joined by zippers, not buttons. However, zippers in initial lymphatics decreased rapidly just before birth, as buttons appeared. The proportion of buttons increased from only 6% at E17.5 and 12% at E18.5 to 35% at birth, 50% at postnatal day (P)7, 90% at P28, and 100% at P70. In inflammation, zippers replaced buttons in airway lymphatics at 14 and 28 days after *Mycoplasma pulmonis* infection of the respiratory tract. The change in lymphatic junctions was reversed by dexamethasone but not by inhibition of vascular endothelial growth factor receptor-3 signaling by antibody mF4-31C1. Dexamethasone also promoted button formation during early postnatal development through a direct effect involving glucocorticoid receptor phosphorylation in lymphatic endothelial cells. These findings demonstrate the plasticity of intercellular junctions in lymphatics during development and inflammation and show that button formation can be promoted by glucocorticoid receptor signaling in lymphatic endothelial cells. *(Am J Pathol 2012, 180:2561–2575; http://dx.doi.org/10.1016/j.ajpath.2012.02.019)*

Lymphatic vessels have long served as transport routes for extravasated fluid, antigens, and immune cells from tissues to lymph nodes and then back into the bloodstream.[1–5] The understanding of this process has evolved in stages. Lymphatics were found many years ago to be sites of tracer uptake,[6,7] but the entry mechanism was unknown until electron microscopic studies in the 1960s and 1970s revealed that lymphatic endothelial cells have open junctions and are coupled to the extracellular matrix by anchoring filaments.[8,9] Elevated interstitial fluid pressure is thought to open the junctions by displacing anchoring filaments.

A subsequent refinement of the mechanism is the concept of a two-valve system in lymphatics for unidirectional entry and movement of fluid and cells.[10] Primary valves in the initial part of lymphatics regulate fluid and cell entry, and secondary valves in collecting lymphatics prevent backflow.[10–12]

The nature of the primary valves is incompletely understood, even though the structure, function, and formation of secondary valves are well characterized.[6,10,13–19] The discovery of discontinuous, button-like junctions (buttons) at the border of oak leaf–shaped endothelial cells of initial lymphatics sheds light on the morphological basis of primary valves.[20,21] The unique structure of these junctions, which are strikingly different from continuous zipper-like junctions (zippers) in other parts of lymphatics, led to the concept that fluid and cells enter through flap-covered openings between adjacent buttons.[20] The route of dendritic cell entry into lymphatics, viewed by live cell imaging, is consistent with this concept.[22,23]

Little is known about how and when buttons form, whether they change under conditions in which lymphatic function is impaired, and whether the changes are reversible. A clue came from the finding that endothelial cells of new lymphatics that grow at sites of inflammation

Supported by a postdoctoral fellowship award from the Lymphatic Research Foundation (L.-C.Y.) and, in part, by grants from the National Heart, Lung, and Blood Institute (HL-24136 and HL-59157 to D.M.M.).

Accepted for publication February 9, 2012.

Supplemental material for this article can be found at *http://ajp.amjpathol.org* or at *http://dx.doi.org/10.1016/j.ajpath.2012.02.019*.

Address reprint requests to Donald M. McDonald, M.D., Ph.D., Department of Anatomy, University of California, 513 Parnassus Ave., Room S1349, San Francisco, CA 94143-0452. E-mail: donald.mcdonald@ucsf.edu.

are joined by zippers instead of buttons.[20] If growth or remodeling of lymphatics in inflamed tissues is accompanied by loss of primary valves and appearance of continuous junctions that are less permeable, the changes could impair fluid entry and drainage. In airway inflammation, this impairment could contribute to mucosal edema and airflow obstruction, which are common features.[24,25] Although edema commonly results from vascular leakage,[26,27] impaired fluid clearance through lymphatics would amplify any mismatch between the amounts of leakage and clearance.[28–35]

With this background, we sought to learn how and when buttons form in lymphatics during development, to explore the plasticity of buttons in inflammation, and to determine the reversibility of the inflammatory changes. In particular, we asked whether buttons form *de novo* as lymphatics develop, whether buttons transform into zippers in inflammation, and whether the transformation is reversible.

We examined the development of lymphatic endothelial junctions in lymph sacs and in lymphatic vessels in mouse airways and diaphragms from E12.5 to birth and into adulthood.[36,37] We also examined the changes in lymphatic junctions in inflamed airways after *Mycoplasma pulmonis* infection,[20] where lymphangiogenesis is a prominent feature.[29] We tested the reversibility of changes in lymphatic junctions after infection by using dexamethasone to reverse the inflammatory response to *M. pulmonis* infection[38,39] or by blocking vascular endothelial growth factor receptor (VEGFR)-3 signaling to suppress lymphatic growth.[29] Finally, we determined whether dexamethasone can promote button formation through direct effects on glucocorticoid receptor (GR) activation in lymphatic endothelial cells of neonatal mice in the absence of inflammation.[40]

We found that zippers were present at E12.5 and preceded the appearance of buttons in lymphatics during development. Transformation from exclusively zippers to predominately buttons began at E17.5, progressed rapidly at birth, and was 90% complete at P28. Buttons reverted into zippers in sustained inflammation, but treatment with dexamethasone promoted the reappearance of buttons. Dexamethasone also advanced button formation during early postnatal development through a direct effect on lymphatic endothelial cells.

Materials and Methods

Mice

C57BL/6 mice (Charles River, Hollister, CA) of either sex were housed under barrier conditions until they were studied at the desired age. FVB/N mice from the same vendor were bred, and neonates were used in some experiments, as described. Embryonic age was counted from the day of vaginal plug discovery, E0.5. In studies of inflammation, pathogen-free, 8-week-old, female C57BL/6 mice were housed under barrier conditions before and after *M. pulmonis* infection. The Institutional Animal Care and Use Committees of the University of California at San Francisco approved all experimental procedures.

M. pulmonis *Infection*

The C57BL/6 mice were briefly anesthetized (ketamine, 83 mg/kg, and xylazine, 13 mg/kg, by i.m. injection) and then were infected by intranasal inoculation of 50 μL of broth containing 10^6 colony-forming units of *M. pulmonis* organisms of strain CT7.[29] From 7 to 28 days after infection, mice were anesthetized and perfused through the heart with 1% paraformaldehyde (PFA) fixative in PBS (pH 7.4). The tracheas, lungs, and bronchial lymph nodes were removed. The wet weights of lungs and bronchial lymph nodes, expressed as a percentage of final body weight, were used to estimate disease severity.

Dexamethasone Treatment

Adult C57BL/6 mice received dexamethasone (10 mg/kg, i.p.; Phoenix Pharmaceuticals Inc., Belmont, CA) or the same volume of sterile 0.9% NaCl (vehicle)[39] once daily on days 14 through 28 after infection. Newborn C57BL/6 or FVB/N mice (P0) received dexamethasone daily (1 mg/kg, s.c.)[41] or no treatment for 4 days.

Inhibition of VEGFR-3 Signaling

Function-blocking, rat monoclonal anti-VEGFR-3 antibody (clone mF4-31C1; ImClone Systems, Inc., New York, NY) was injected i.p. into 8-week-old, pathogen-free or infected C57BL/6 mice at an initial dose of 2 mg per mouse and then 0.8 mg per mouse every other day for 14 days.[29] In the infected mice, the 14-day treatment began 14 days after infection. PBS was used as a control (vehicle) to treat infected or pathogen-free mice.

IHC Data

Pregnant females were anesthetized (ketamine, 83 mg/kg, and xylazine, 13 mg/kg, i.m.) at timed gestation, and the uterus was opened. E12.5 embryos were removed and fixed by immersion in 4% PFA in PBS at room temperature for 2 hours, cryoprotected with 30% sucrose in PBS, and embedded in Tissue-Tek optimal cutting temperature (OCT) compound (Sakura Finetek, Torrance, CA).[42] Older embryos were euthanized by immersion in ice-cold PBS for 30 minutes without exposure to room air, and then the trachea, lung, and diaphragm were removed in PBS and fixed by immersion in 1% PFA in PBS at room temperature for 1 hour.[43] Mice at P0 and older were anesthetized by injection of the same anesthetic, and the vasculature was fixed by systemic vascular perfusion of 1% PFA in PBS for 2 minutes, followed by immersion of the trachea and diaphragm in the same fixative at room temperature for 1 hour.[43] For ease of making flat whole mounts, the trachea of mice at E16.5 to P7 was cut along the dorsal longitudinal axis; the trachea from adult mice was cut along the ventral longitudinal axis.

Tissue whole mounts or cryostat sections (60-μm thick) were stained by immunohistochemical (IHC) procedures previously described,[43] using the following primary antibodies. For intercellular junctions, we used VE-cadherin [rat anti-mouse, clone 11D4.1 (BD Biosci-

ences, San Jose, CA); goat polyclonal (Santa Cruz, Santa Cruz, CA) was used for tissues from mice treated with the rat anti-VEGFR-3 antibody, in which the anti-rat secondary antibody gave strong background staining]; β-catenin (rabbit polyclonal; Sigma-Aldrich, St. Louis, MO); p120-catenin (rabbit anti-mouse, clone E205; Epitomics, Burlingame, CA); and zonula occludens protein 1 (ZO-1), occludin, and/or claudin-5 (rabbit polyclonal; Invitrogen, Carlsbad, CA). For lymphatics, we used lymphatic vessel endothelial cell receptor (LYVE)-1 [rabbit polyclonal (AngioBio, Del Mar, CA) or goat polyclonal (R&D, Minneapolis, MN)], Prox1 [rabbit polyclonal (AngioBio) or goat polyclonal (R&D)], and/or podoplanin (Syrian hamster anti-mouse, clone 8.1.1; eBioscience, San Diego, CA). For activated GR, we used phosphorylated (phospho)-GR (Ser211, rabbit polyclonal; Cell Signaling, Danvers, MA). Primary antibodies were identified by secondary antibodies labeled with fluorescein isothiocyanate, Cy3, or Cy5 (Jackson ImmunoResearch, West Grove, PA). Specimens were viewed with a Zeiss Axiophot fluorescence microscope or a Zeiss LSM-510 confocal microscope (Carl Zeiss, Oberkochen, Germany) using AIM 4.0 confocal software (Carl Zeiss).

Morphometric Measurements

Lymphatics in whole mounts of trachea and diaphragm were measured in real-time images by using a digitizing tablet linked to a video camera on a Zeiss Axiophot microscope. For the quantitative studies, buttons were defined as distinct, discontinuous segments of VE-cadherin immunoreactivity at the border of endothelial cells of initial lymphatics. Zippers were defined as distinct, continuous lines of VE-cadherin at cell borders. Junctions that were not clearly recognized as either buttons or zippers were designated intermediate junctions.

The number of VE-cadherin–stained buttons per 1000-μm^2 projected area of LYVE-1–stained lymphatic vessel surface was measured at a final screen magnification of 1520 (surface density of buttons). In the trachea, one lymphatic was measured in each of 5 to 10 spaces between cartilage rings, beginning at the rostral end near the larynx. In the diaphragm, 5 to 10 lymphatics in the central tendon were measured. Embryonic data were obtained from two or more litters.

Age-related changes in the proportions of zippers, buttons, and intermediate junctions (proportion of total junctions) were assessed by examining the frequency of each junctional type in tracheal lymphatics from E16.5 to adult (P70). Measurements of the surface density of buttons were used as the reference at each age, and the total amount of junctional length per cell was considered 100%. The size and perimeter of lymphatic endothelial cells were relatively constant.

For the time course of zipper-to-button transformation after infection, we examined 5 to 10 regions of the trachea of each of five mice per group after 7, 14, or 28 days of infection. Sprouts and stalks of new lymphatics were measured over cartilage rings, where none are present normally; and existing lymphatics were measured between cartilage rings, where lymphatics are normally located. The area density of LYVE-1–positive vessels was measured by stereological point counting at a final screen magnification of 960[29] in regions of mucosa over cartilage rings (one region per ring; 10 rings per mouse), where the changes during infection were greatest.

Statistical Analysis

Values are presented as mean ± SEM, with 5 to 10 mice per group. Differences between means were assessed by analysis of variance, followed by the Bonferroni test for multiple comparisons. $P < 0.05$ was considered significant.

Results

Zippers between Endothelial Cells of Primitive Lymphatic Structures at E12.5

Jugular lymph sacs are primitive lymphatic structures that derive from a population of Prox1-expressing cells of the anterior cardinal vein and produce lymphatic vessels.[44] To determine whether intercellular junctions are present and specifically whether buttons are present when lymphatics form, we examined Prox1-positive cells in the anterior cardinal vein, jugular lymph sacs, and neighboring lymphatic structures (Figure 1, A–D). At E12.5, Prox1 cells budding from the anterior cardinal vein were joined exclusively by zippers, which were identified as continuous lines of VE-cadherin immunoreactivity at cell borders (Figure 1B). No buttons were found. Similarly, Prox1 cells in jugular lymph sacs and adjacent lymphatic structures had zippers (Figure 1, C and D). Small clusters of apparently migrating Prox1 cells (Figure 1, E and F) were also joined by zippers similar to those in growing blood vessels (Figure 1G). More than 90% of Prox1 cells examined in cross sections of E12.5 embryos were interconnected by zippers marked by VE-cadherin immunoreactivity.

The trachea and lungs develop by growth and branching of endodermal epithelium into the surrounding mesenchyme around E11 in the mouse.[45] An examination of whole mounts of trachea and lung at E12.5 revealed that the primary blood vascular network was already established in the lungs and formed a primitive plexus in the trachea (Figure 1H). Prox1 cells were abundant in the trachea and were arranged in primitive networks, unlike the segmental pattern at birth and beyond. Prox1 cells in the lung were distributed along the main stem and secondary bronchi. At this early stage, tracheal lymphatics and some blood vessels had VEGFR-3 immunoreactivity, but LYVE-1 staining was faint or absent (data not shown). Endothelial cells of the tracheal lymphatic plexus had zippers, shown by VE-cadherin staining, but no buttons (Figure 1, I and J).

Zipper-to-Button Transformation in Initial Lymphatics around Birth

The tracheal mucosa of adult mice has a distinctive segmental arrangement of lymphatics, which are restricted to regions between cartilage rings and are largely absent over the cartilage rings.[20,39] Unlike the primitive plexus at E12.5, tracheal lymphatics at E16.5 had a segmental pattern of

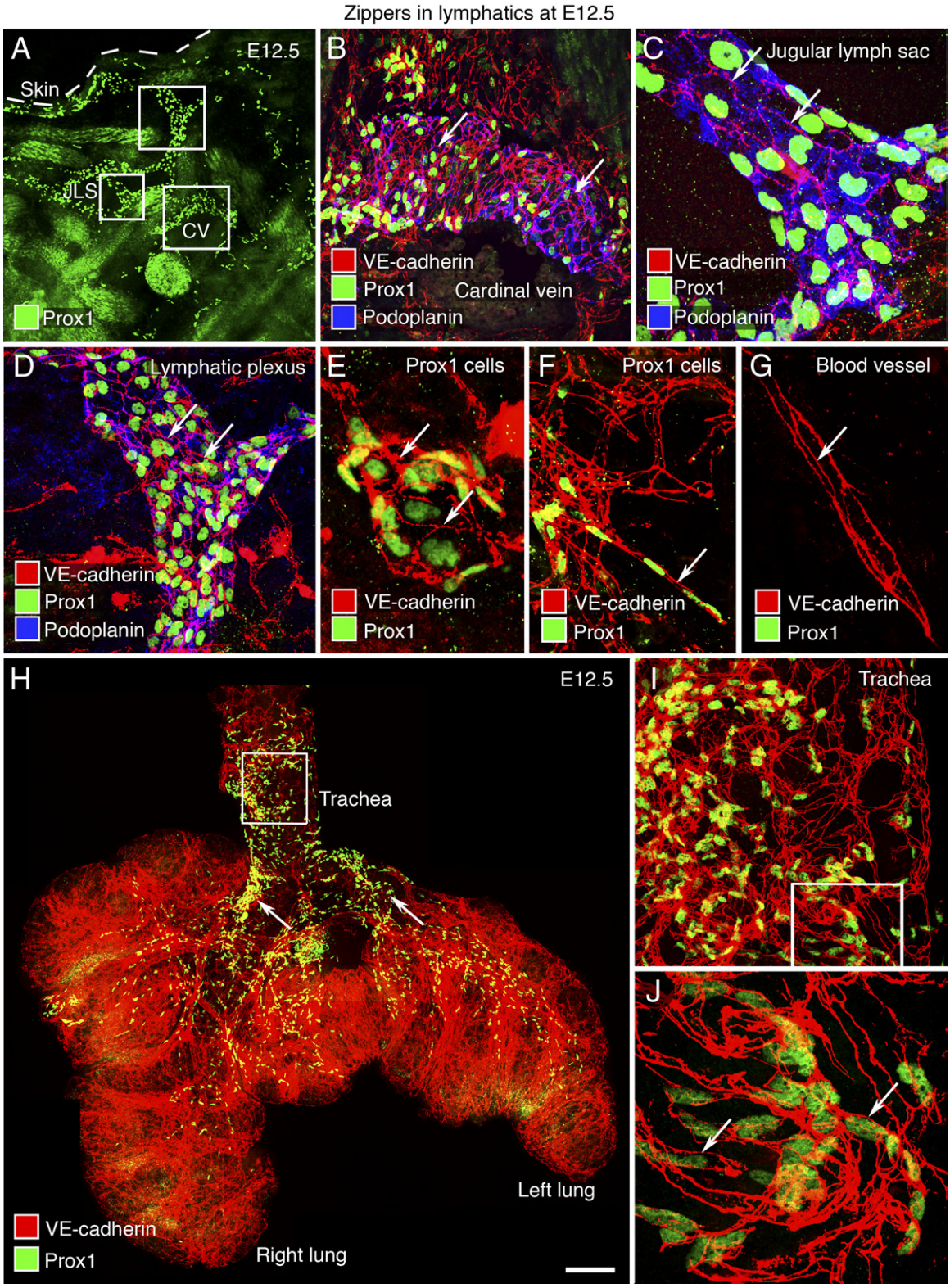

Figure 1. Zipper-like junctions in primitive lymphatic endothelium at E12.5. **A:** Low-magnification view of Prox1-immunoreactive endothelial cell nuclei (green) in a cross section of embryo at E12.5 showing the anterior cardinal vein (CV), jugular lymph sac (JLS), and tissue near the JLS. Boxed regions in **A** are enlarged in **B–D**. **B–D:** Endothelial cells joined by zippers (**arrows**) in lymphatic structures stained for Prox1 (green) and podoplanin (blue) are shown next to the cardinal vein (**B**), within the JLS (**C**), and in adjacent tissue (**D**). **E** and **F:** Zippers (**arrows**) in a cluster of Prox1-positive endothelial cells. **G:** Zippers (**arrow**) in the endothelium of a blood vessel (Prox1 negative) at E12.5. **H–J:** Whole mount of trachea and lungs at E12.5 showing zippers in the endothelium (VE-cadherin, red) of blood vessels and lymphatics and nuclei of lymphatic endothelial cells (Prox1, green). **Arrows**, main stem bronchi. The boxed region in **H** is enlarged in **I** to show the primitive lymphatic plexus in the trachea. The boxed region in **I** is enlarged in **J**, as well as a small region outside the field of view, to show zippers in the endothelium of lymphatics at E12.5 (**J: arrows**). Scale bars: 200 μm (**A**); 50 μm (**B**, **D**, and **I**); 20 μm (**C**, **E–G**, and **J**); 400 μm (**H**).

interconnected vessels between cartilage rings. Tracheal lymphatics at E16.5 resembled the adult pattern but had little branching (Figure 2A), and the endothelial cells were joined by zippers (Figure 2A), not buttons.

Buttons, identified as segments of VE-cadherin staining, which appeared to be oriented perpendicular to the endothelial cell border, were first detected in tracheal lymphatics at E17.5 and became more abundant thereafter (Figure 2, B–L). Measurements made to determine the rate of appearance of buttons during the development of tracheal lymphatics revealed that the relative frequency of buttons was 6% at E17.5, 12% at E18.5, 35% at birth (P0), 50% at P7, 62.5% at P14, and 90% at P28; the number of buttons per initial lymphatic in the adult (P70) served as the reference (Figure 2B).

To determine whether values from the trachea applied to other organs, we measured the appearance of buttons in initial lymphatics of the diaphragm[20] and obtained relatively similar values. Compared with values in the adult, buttons in diaphragmatic lymphatics had a frequency of 1% at E17.5, 4% at E18.5, 20% at P0, 50% at P7, 60% at P14, and 81% at P28 (Figure 2B). During the day of birth, between E18.5 and P0, buttons became twice as abundant in the trachea and four times as numerous in the diaphragm. Zippers in the endothelium of collecting lymphatics were unchanged during this period.

A more detailed examination of the apparent transformation of zippers into buttons revealed that the junctions between lymphatic endothelial cells could not meaningfully be divided into only two distinct categories. Intermediate forms were present (Figure 2, C–L). We divided the process of button formation into four stages (Figure 2, D–L). First, from E17.5 to E18.5, VE-cadherin at cell borders changed conspicuously from uniform lines to lines with alternating thick and thin regions (Figure 2, D and I). Second, from P0 through P7, some cell junctions appeared fragmented, whereas others did not appear fragmented; most cell borders were smooth (Figure 2, E and J). Third, from P7 to P14, buttons were more distinct, the border of some cells was scalloped, and the cells had an oak leaf shape (Figure 2, F and K). The apparent perpendicular orientation of buttons coincided with the appearance of the scalloped border of oak leaf–shaped endothelial cells. Fourth, after P14, buttons marked by VE-cadherin staining had the distinctive adult pattern, and the endothelial cells of most initial lymphatics were oak leaf shaped (Figure 2, G and L). At three-cell junctions, buttons had a distinctive three-part structure resembling a three-bladed propeller (Figure 2, G and L).

The stages were similar in the trachea and diaphragm but were easier to analyze in the diaphragm. Buttons counted in Figure 2B were distinctly segmented junctions. Intermediate forms of junctions were the most prevalent type from P0 through P14 but were counted as buttons only if they had distinct button-like segments.

During this period, changes in the distribution of LYVE-1 in lymphatic endothelial cells coincided with changes in VE-cadherin. At E16.5, LYVE-1 immunoreactivity was uniformly spread over the surface of endothelial cells (Figure 2H). From E17.5 to E18.5, some LYVE-1 was dispersed and some was concentrated at cell borders (Figure 2I). From P0 through P7, LYVE-1 was consistently more concentrated near buttons (Figure 2J). From P7 to P14, LYVE-1 was strong at cell borders, where it was located between buttons and had a complementary distribution to VE-cadherin (Figure 2K). After P14, the complementary patterns of LYVE-1 and VE-cadherin highlighted the distinctive oak leaf shape of endothelial cells of initial lymphatics in the adult (Figure 2L).[20,46]

To compare the age-related changes in zippers, intermediate junctions, and buttons, we estimated the proportions of each type of junction in the trachea from E16.5 to P70 (Figure 2M). The incidence of zippers decreased steeply just before birth to only 20% of the value at E16.5. Intermediate junctions increased rapidly just before birth and then gradually decreased during the next four weeks as they transformed into buttons. Buttons appeared just before birth, but at P0, they represented only about 30% of the eventual number in initial lymphatics at P70. Even at P70, approximately 5% of the junctions in initial lymphatics had the form of zippers or intermediate junctions.

Junctional Proteins in Lymphatic Endothelial Cells at Different Developmental Stages

With evidence that VE-cadherin is a consistent feature of endothelial cell junctions in lymphatics throughout development and in the adult,[20,47] we sought to determine whether other junctional proteins make similarly constant contributions as zippers transform into buttons. We found that the intensity of IHC staining for the tight junction proteins claudin-5, occludin, and ZO-1 (an intracellular partner that interacts with the actin cytoskeleton) was similar at E17.5, P0, and P28 in zippers, buttons, and intermediate-type junctions (see Supplemental Figures S1 and S2 at *http://ajp.amjpathol.org*).[20,47] The intracellular proteins β-catenin and p120-catenin, which play an important role in stabilizing endothelial cell-cell adhesion by linking VE-cadherin to the actin cytoskeleton,[47] colocalized with VE-cadherin at E17.5 and P0 in all three types of junctions (Figure 3, A–H).

Button-to-Zipper Transformation in Lymphatics after M. pulmonis *Infection*

To build on evidence that zippers predominate in growing sprouts from initial lymphatics at sites of inflammation,[20] we asked whether all newly formed lymphatics have zippers, as in early development, or whether this change is a manifestation of the transformation of buttons to zippers in a pathological setting. Our approach was to compare the distribution of buttons and zippers in tracheal lymphatics after *M. pulmonis* infection for 7, 14, or 28 days, with that present normally.

In tracheas of pathogen-free adults, lymphatics were restricted to regions of mucosa between cartilage rings (Figure 4A). As previously reported,[20] buttons identified by discontinuous VE-cadherin immunoreactivity at the scalloped border of lymphatic endothelial cells were present in 100% of initial lymphatics (Figure 4B), but not in collecting lymphatics, which had zippers (Figure 4C).

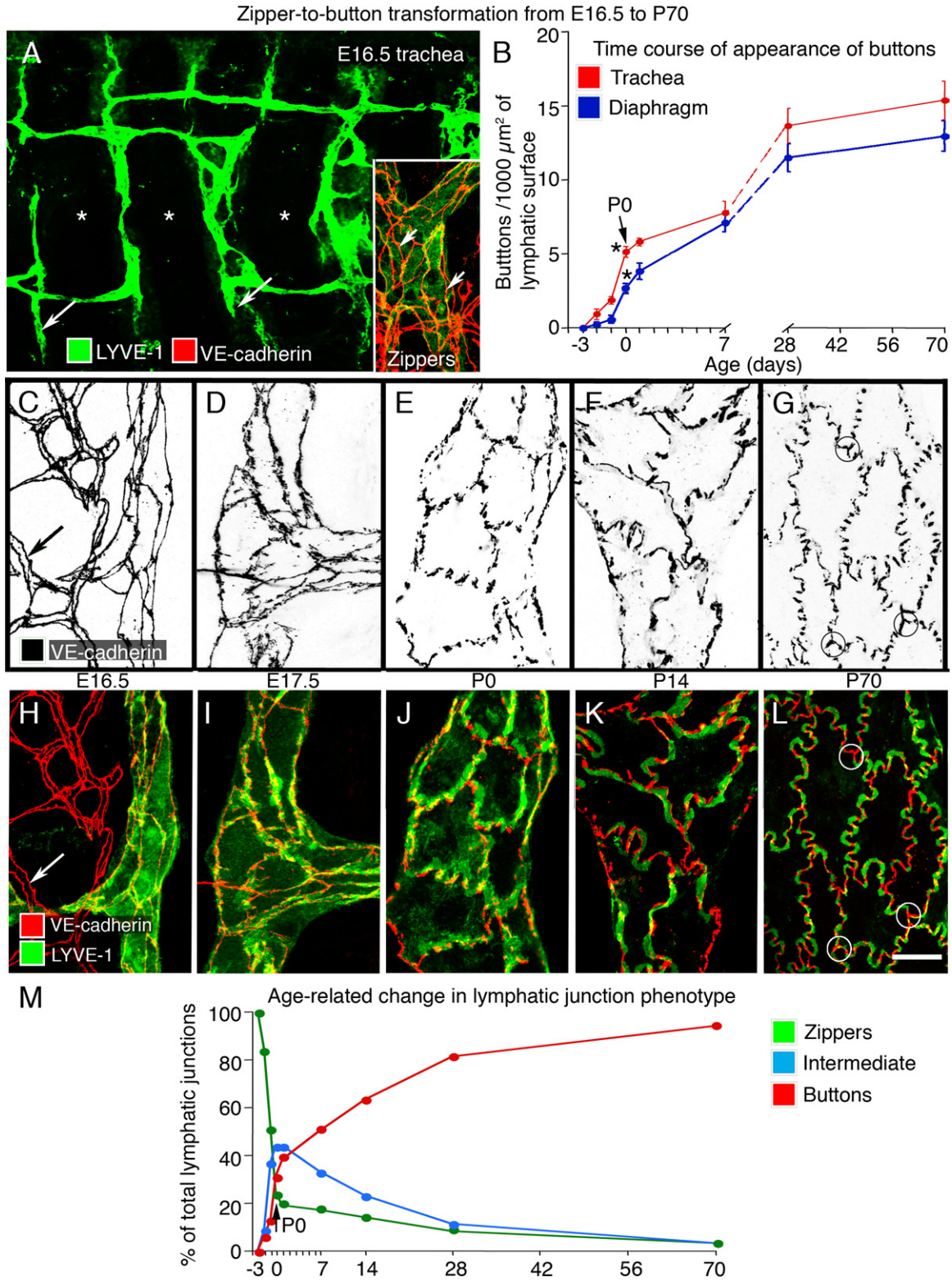

Figure 2. Development of button-like junctions in the endothelium of lymphatics. **A:** Lymphatic vascular plexus (LYVE-1, green) in a tracheal whole mount at E16.5, showing tips of initial lymphatics (**long arrows**). **Inset:** Zipper-like junctions (VE-cadherin, red) in lymphatic endothelium (**short arrows**). Most of the lymphatics are located between cartilage rings (**asterisks**). **B:** Time course of development of button-like junctions in lymphatics of trachea (red) and diaphragm (blue) from E16.5 to P70. Buttons are expressed as number of adult-like VE-cadherin–stained segments. Buttons that appear before birth represent only approximately 35% and 20% of the eventual number present in adult (P70) initial lymphatics of trachea and diaphragm, respectively. $^*P < 0.05$, values at P0 (**arrow**) are significantly different from those at E18.5. **C–L:** Lymphatic endothelial cell junctions are shown as inverted gray scale images (**C–G:** VE-cadherin) and in color (**H–L:** VE-cadherin, red; LYVE-1, green) to illustrate the sequence of changes in zipper-to-button transformation from E16.5 to P70 (diaphragm). Zippers are also shown in a blood vessel at E16.5 (**C** and **H: long arrow**). At P70, a distinctive structure at the junction of three lymphatic endothelial cells with button-like junctions is indicated by circles (**G** and **L**). **M:** Changes of tracheal lymphatic junction phenotype from E16.5 to P70, including zippers (green), intermediate (light blue), and buttons (red). Scale bars: 100 μm (**A**); 10 μm (**C–L**).

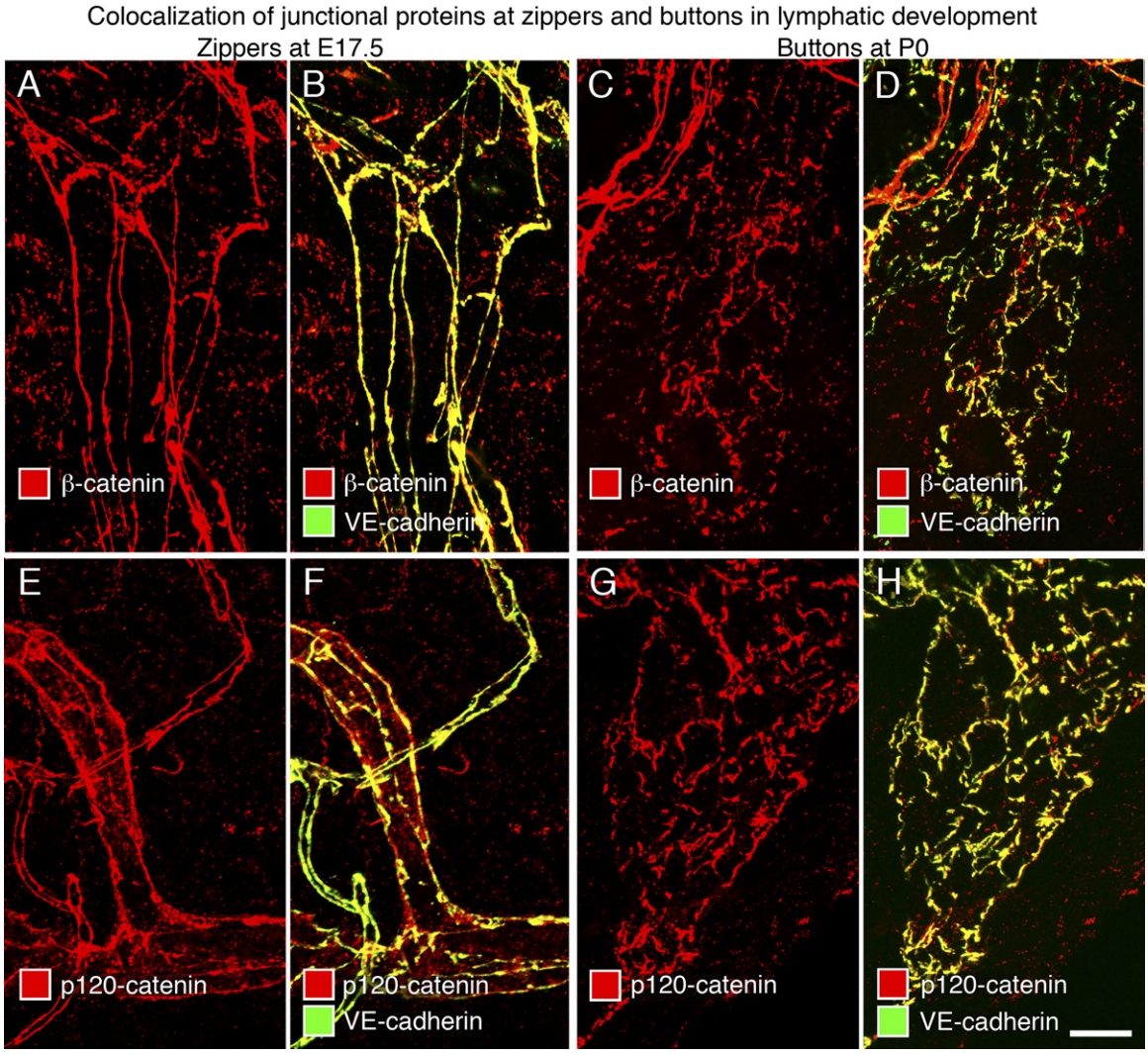

Figure 3. Colocalization of β-catenin and p120-catenin with VE-cadherin at lymphatic endothelial cell junctions at E17.5 and P0. Confocal images of tracheal lymphatics showing colocalization of β-catenin (**A–D**) or p120-catenin (**E–H**) (red) and VE-cadherin (green) at zippers at E17.5 (**A**, **B**, **E**, and **F**) and at primitive buttons at P0 (**C**, **D**, **G**, and **H**). Junctions in tracheal lymphatics had clear VE-cadherin immunoreactivity at E17.5 and P0, albeit weaker than in blood vessels. Yellow staining in **B**, **D**, **F**, and **H** reflects the colocalization of VE-cadherin (green) and β-catenin or p120-catenin (red) at junctions in lymphatic vessels. Scale bar = 10 μm.

After *M. pulmonis* infection, new lymphatics were evident at 7 days and were abundant at 14 days (Figure 4D). Lymphatic sprouts were readily identified in regions over cartilage rings, because no lymphatics were normally present. At 7 days, zippers were present in lymphatic sprouts over the rings, suggesting that they were present as the sprouts grew. Buttons still predominated in initial lymphatics between the rings at 7 days, but 50% of these lymphatics had zippers at 14 days and 75% had zippers at 28 days, indicating that zippers gradually replaced buttons in the existing initial lymphatics.

Staining of lymphatic sprouts for the tight junction protein claudin-5 after 14 days of infection gave essentially the same number and distribution of zippers as did staining for VE-cadherin (Figure 4, E and F). The same was found for zippers in other regions of initial lymphatics, where buttons would normally be found (Figure 4, G–I). This feature of the junctional composition of zippers after infection resembled that observed under normal conditions.

Reversal of Button-to-Zipper Transformation in Infected Airways

Because buttons appeared to transform into zippers after infection, we asked whether the process was reversible. We used two approaches. First, we determined whether the zippers could be reverted to buttons by reducing the inflammation by treatment with dexamethasone, which decreases the severity of *M. pulmonis* infection and reduces VEGFR-3 expression in infected airways.[29,39] Second, we reduced VEGF-C–mediated lymphangiogenesis after infection by treatment with the function-blocking anti-VEGFR-3 antibody mF4-31C1.[29,39]

Treatment of adult mice with dexamethasone for 14 days was started after infection was established for 14 days, when new lymphatics were abundant in the trachea. As previously reported,[29,39] dexamethasone treatment stopped further lymphangiogenesis but did not

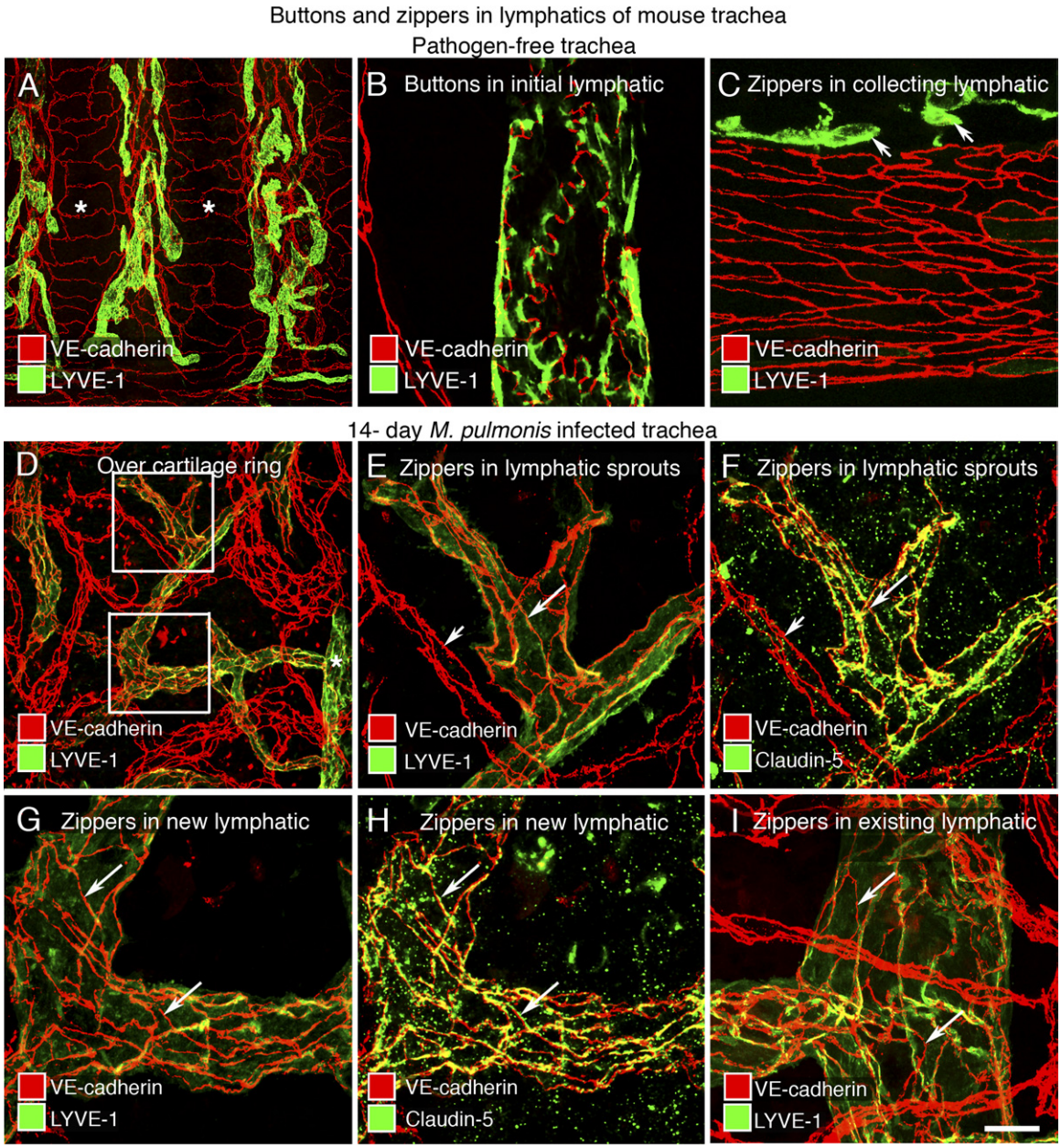

Figure 4. Transformation of buttons to zippers in lymphatics after *M. pulmonis* infection. Confocal images of lymphatics in tracheal whole mounts of pathogen-free or *M. pulmonis*–infected mice. **A–C:** Different distributions of lymphatics (LYVE-1, green) and blood vessels (VE-cadherin, red) in pathogen-free trachea. Regions of mucosa over cartilage rings (**asterisks**) are almost free of lymphatics (**A**). VE-cadherin (red) and LYVE-1 (green) have complementary distributions at buttons in initial lymphatics (**B**), but LYVE-1 is weak or absent in collecting lymphatics (**C**). Some extracellular leukocytes also have LYVE-1 immunoreactivity (**C: short arrows**). **D–I:** Zippers in lymphatic endothelium shown after *M. pulmonis* infection (14 days) by staining for VE-cadherin (red) and LYVE-1 (**D**, **E**, **G**, and **I**) or claudin-5 (**F** and **H**) (green). Network of new or remodeled lymphatics above a cartilage ring (**D**). The boxed regions in **D** are enlarged in **E–H** to show zippers. **E–I:** Zippers (**long arrows**) in tips of lymphatic sprouts (**E** and **F**), stalks of lymphatic sprouts (**G** and **H**), and other regions of remodeled initial lymphatics (**I**). Claudin-5 is weak in blood vessels (**E** and **F: short arrow**). Scale bars: 200 μm (**A**); 50 μm (**D**); 20 μm (**B**, **C**, and **E–I**).

cause regression of new lymphatics that had grown over cartilage rings (Figure 5A). As a measure of disease severity, the treatment reduced by 85% the 22-fold weight gain of bronchial lymph nodes and reduced by 53% the threefold weight gain of lungs at 28 days after infection (Figure 5B).

In contrast to tracheas of mice infected for 28 days without treatment, in which zippers were abundant in lymphatics (Figure 5, C–E), buttons predominated in lymphatics of infected mice treated with dexamethasone for the final 14 days (Figure 5, F–H). Similar effects of dexamethasone were found on the distribution of LYVE-1 in lymphatic endothelial cells. The uniform distribution of LYVE-1 staining in lymphatics after infection changed after dexamethasone into a pattern in which staining was concentrated at endothelial cell borders at sites between VE-cadherin–stained buttons (Figure 5, F–H). These effects of dexamethasone were consistent with promotion of button formation, redistribution of LYVE-1, and recovery of the oak leaf phenotype of lymphatic endothelial cells.

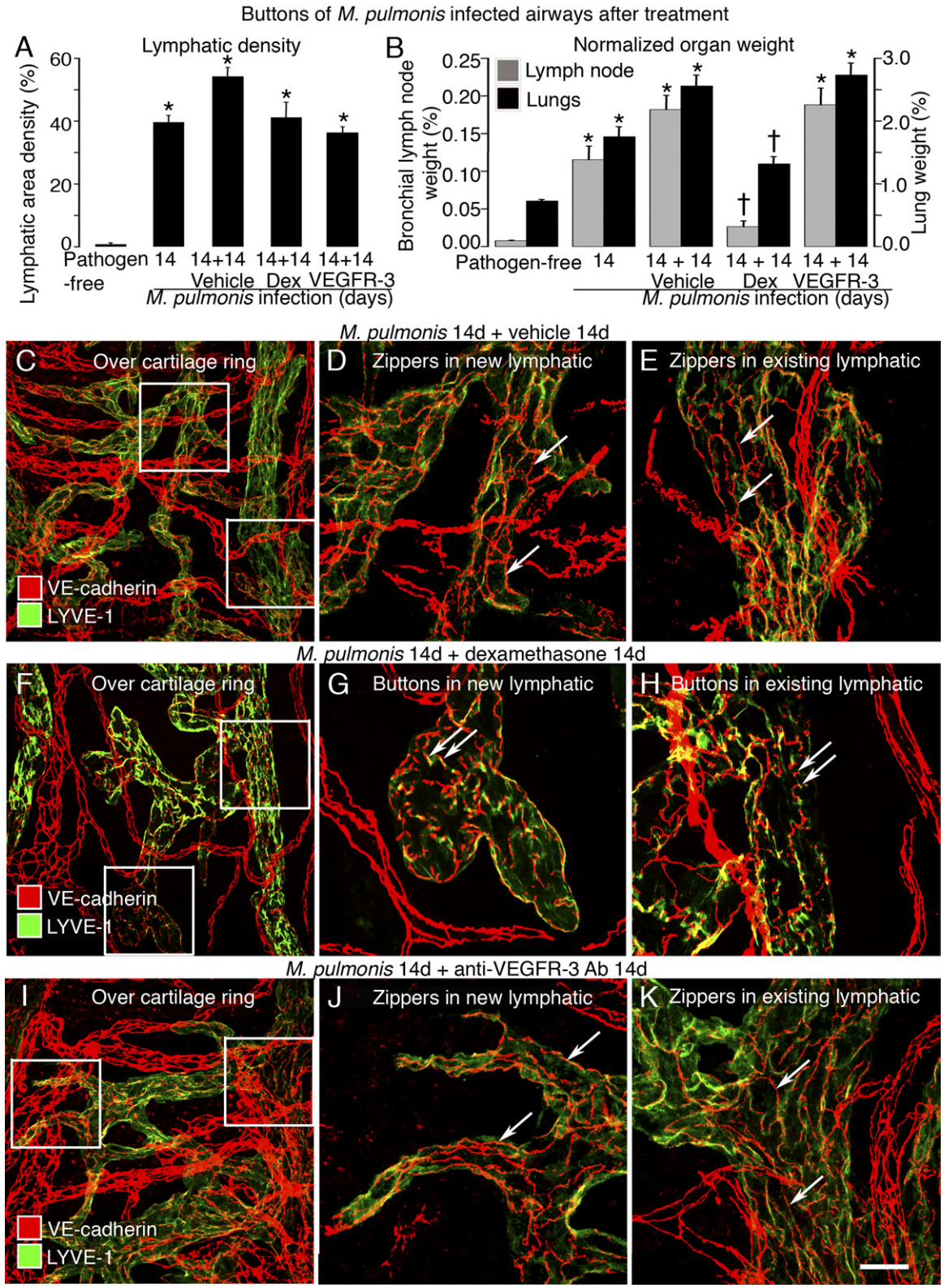

Figure 5. Reversal of button-to-zipper conversion in inflamed airways. **A** and **B:** Lymphatic area density in mucosa overlying cartilage rings (**A**) and normalized bronchial lymph node and lung weights (**B**). $^{*}P < 0.05$ versus pathogen-free mice; $^{\dagger}P < 0.05$ versus the 14-day infected baseline group. Dex, dexamethasone. **C–E:** Zippers in lymphatic endothelium shown after *M. pulmonis* infection and vehicle treatment by staining for VE-cadherin (red) and LYVE-1 (green). Enlargement of boxed regions in **C** shows zippers (**arrows**) in both new (**D**) and existing (**E**) lymphatics. **F–H:** Buttons in nonregressed lymphatic endothelium shown after *M. pulmonis* infection and Dex treatment. Enlargement of boxed regions in **F** shows buttons (**arrows**) in the oak leaf–shaped endothelial cells of new (**G**) and existing (**H**) lymphatics. **I–K:** Zippers (**arrows**) in lymphatic endothelium shown after *M. pulmonis* infection and anti-VEGFR-3 antibody treatment. Enlargement of boxed regions in **I** shows zippers (**arrows**) in both new (**J**) and existing (**K**) lymphatics. Scale bars: 50 μm (**C**, **F**, and **I**); 20 μm (**D**, **E**, **G**, **H**, **J**, and **K**).

To determine whether zipper formation after infection is driven by VEGFR-3 signaling, we blocked VEGFR-3 signaling with the antibody mF4-31C1 from day 14 to 28 after infection of adult mice. This treatment prevented further lymphangiogenesis but did not reduce the density of tracheal lymphatics to less than the amount present at the onset of treatment (Figure 5A) and did not block the infection-related weight gain of bronchial lymph nodes and lungs (Figure 5B). Unlike dexamethasone, mF4-31C1 treatment did not reduce the proportion of zippers in lymphatic sprouts or stalks (Figure 5, I–K). Control experiments in tracheas of 8-week-old pathogen-free mice showed that mF4-31C1 for 2 weeks did not alter the number or appearance of buttons in normal initial lymphatics (data not shown).

Promotion by Dexamethasone of Zipper-to-Button Transformation in Neonatal Airways

Next, we examined the question of whether the promotion of zipper-to-button conversion by dexamethasone results from anti-inflammatory actions of dexamethasone or from a direct effect on lymphatics. These experiments exploited the natural zipper-to-button transformation that occurs in neonatal airways from P0 to P4. The approach was to determine whether dexamethasone accelerated this natural transformation in neonates.

We found that the overall organization of lymphatics in the trachea of mice treated with dexamethasone from P0 to P4 was similar to that of nontreated littermates (Figure 6, A and B). However, individual lymphatics after dexamethasone had striking differences from the nontreated controls. In healthy neonates at P4, most junctions in initial lymphatics were intermediate between zippers and buttons, except for lymphatic sprouts, where zippers predominated (Figure 6, A, C, and D); lymphatic endothelial cells had an irregular shape and a uniform distribution of LYVE-1 (Figure 6, A and D). In contrast, initial lymphatics in dexamethasone-treated neonates at P4 had lymphatics with ubiquitous buttons resembling those in the adult (Figure 6E) and few intermediate junctions. The lymphatics were wider, had more rounded ends, and had few sprouts or zippers (Figure 6B). The endothelial cells of these lymphatics were oak leaf shaped, and the distribution of LYVE-1 was complementary to the pattern of VE-cadherin in buttons (Figure 6E). The same results were obtained in a repeat experiment using neonates of the FVB/N background (data not shown).

The promotion of button formation by dexamethasone was restricted to initial lymphatics. Collecting lymphatics, identified by the presence of intraluminal valves, had only zippers (Figure 6, F and G). Also, after dexamethasone, the endothelium of the thoracic duct had only zippers (Figure 6, H and I), albeit the endothelial cell borders were more jagged than those in the controls.

Activation of GRs in Lymphatic Endothelial Cells

To further explore whether dexamethasone promotes button formation in neonates by acting directly on lymphatics, we determined whether lymphatic endothelial cells have GRs and whether dexamethasone activates the receptors. Neonatal C57BL/6 mice were treated with dexamethasone from P0 to P4, and activated GR immunoreactivity was assessed in tracheal lymphatics using an antibody to phospho-GR (Ser211), which accumulates in the nucleus after ligand binding.[48] In untreated neonates at P4, many cell types, including Prox1-positive cells of lymphatics, had detectable nuclear phospho-GR immunoreactivity, but the intensity was variable, and staining was faint in lymphatics with zippers (Figure 7, A and B). However, after dexamethasone, phospho-GR immunoreactivity was uniformly stronger in Prox1-positive nuclei of lymphatic endothelial cells that had buttons (Figure 7, C and D). No nuclear staining was present when the phospho-GR primary antibody was omitted (Figure 7, E and F).

Discussion

This study revealed a previously unrecognized plasticity of intercellular junctions in the endothelium of the initial part of lymphatics, where fluid and cell entry is thought to occur. Zippers transformed into buttons during development, and buttons transformed into zippers in inflammation. When the lymphatic network of the mouse trachea was established at E16.5, only zippers were present. Similar junctions were present in jugular lymph sacs and in the primitive lymphatic plexus of the trachea at E12.5. Zippers began to be replaced by buttons at E17.5. This transformation was rapid at birth and largely complete by P28. No change was found in the composition of the junctional proteins during this transformation. In sustained inflammation after *M. pulmonis* infection, zippers had replaced buttons in existing initial lymphatics by 14 to 28 days. Treatment with dexamethasone reversed the junctional change in inflammation and promoted button formation in neonatal lymphatics. Dexamethasone caused the accumulation of phosphorylated GRs in the nucleus of lymphatic endothelial cells, consistent with a direct action on these cells.

Changes in Lymphatic Endothelial Cell Junctions during Development

The endothelial cells of lymphatic sacs and other primitive lymphatic structures present at E12.5 were joined by zippers. Buttons were not found until late gestation. Most lymphatic endothelial cells identified by Prox1 staining at E12.5 were joined by zippers and were part of multicellular lymphatic sprouts, rather than separate migrating cells.

Several lines of evidence from studies of developing lymphatics were consistent with the concept that buttons form from zippers via intermediate junctional forms. First, zippers, buttons, and intermediate junctions were composed of the same proteins. Second, zippers preceded the appearance of buttons in development. Third, the number of zippers decreased sharply just before birth, precisely when buttons appeared. Fourth, intermediate junctional forms resembled fragmented zippers and were most numerous as buttons increased in abundance around birth, but they were rare in the adult. Fifth, the gradual increase in buttons during the first 4 weeks after birth coin-

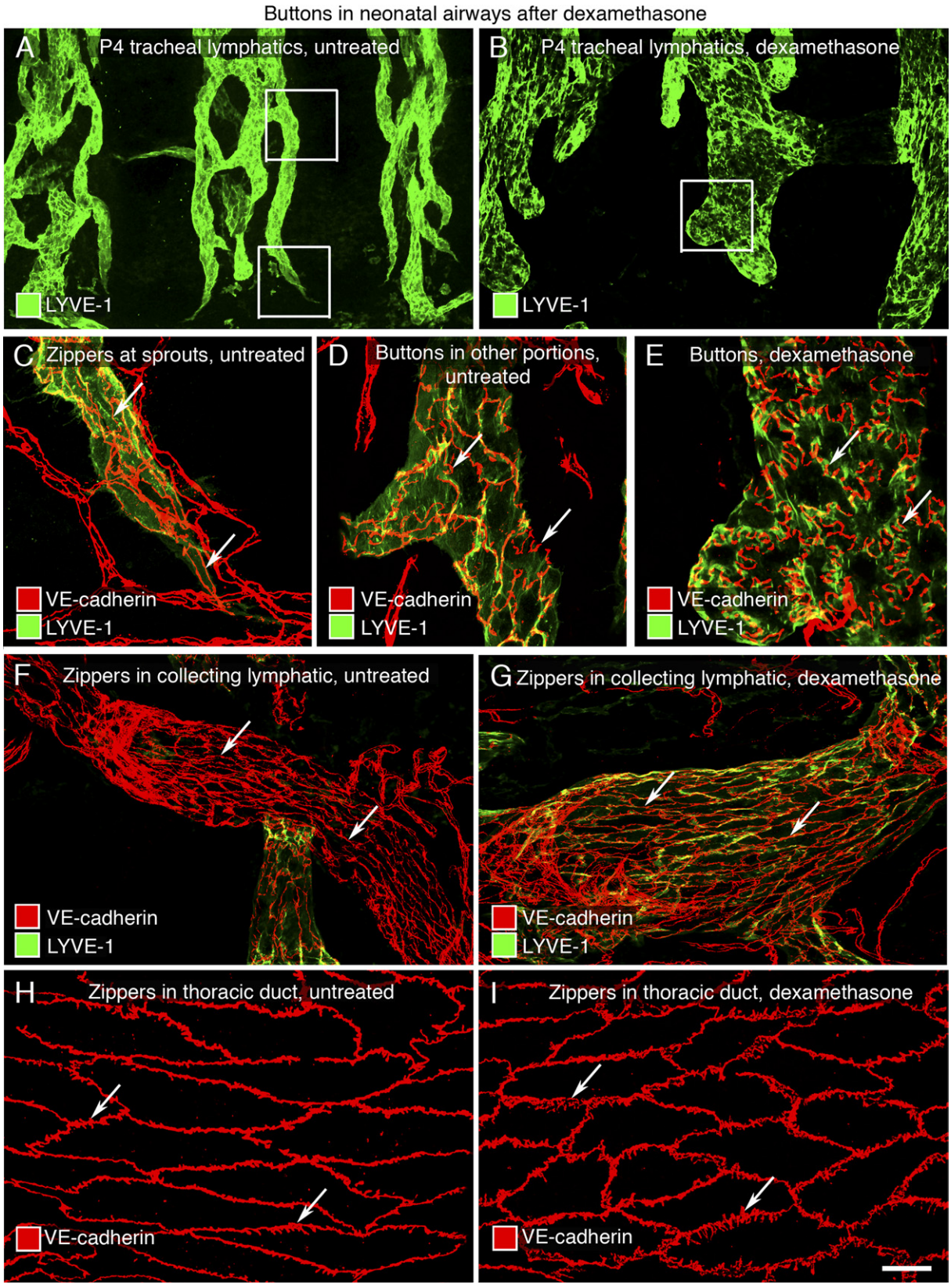

Figure 6. Promotion of button formation in neonatal lymphatics by dexamethasone. **A** and **B:** Lymphatics (LYVE-1, green) in tracheal whole mounts of untreated (**A**) or dexamethasone-treated (**B**) P4 pups. Boxed regions in **A** and **B** are enlarged in **C** and **D**, and **E**, respectively. **C** and **D:** VE-cadherin (red)–stained zippers in tips of lymphatic sprouts (**C: arrows**) and primitive buttons in other portions (**D: arrows**) of initial lymphatics from untreated trachea. **E:** After dexamethasone, oak leaf–shaped endothelial cells have buttons (**arrows**) with a complementary distribution with LYVE-1 (green) at cell borders. **F** and **G:** Zippers (**arrows**) in collecting lymphatics containing intraluminal valves from untreated (**F**) and dexamethasone-treated (**G**) mice. **H** and **I:** Jagged zipper-like junctions (**arrows**) in thoracic ducts of untreated (**H**) and dexamethasone-treated (**I**) mice. Scale bars: 100 μm (**A** and **B**); 50 μm (**F** and **G**); 20 μm (**C**–**E** and **H**–**I**).

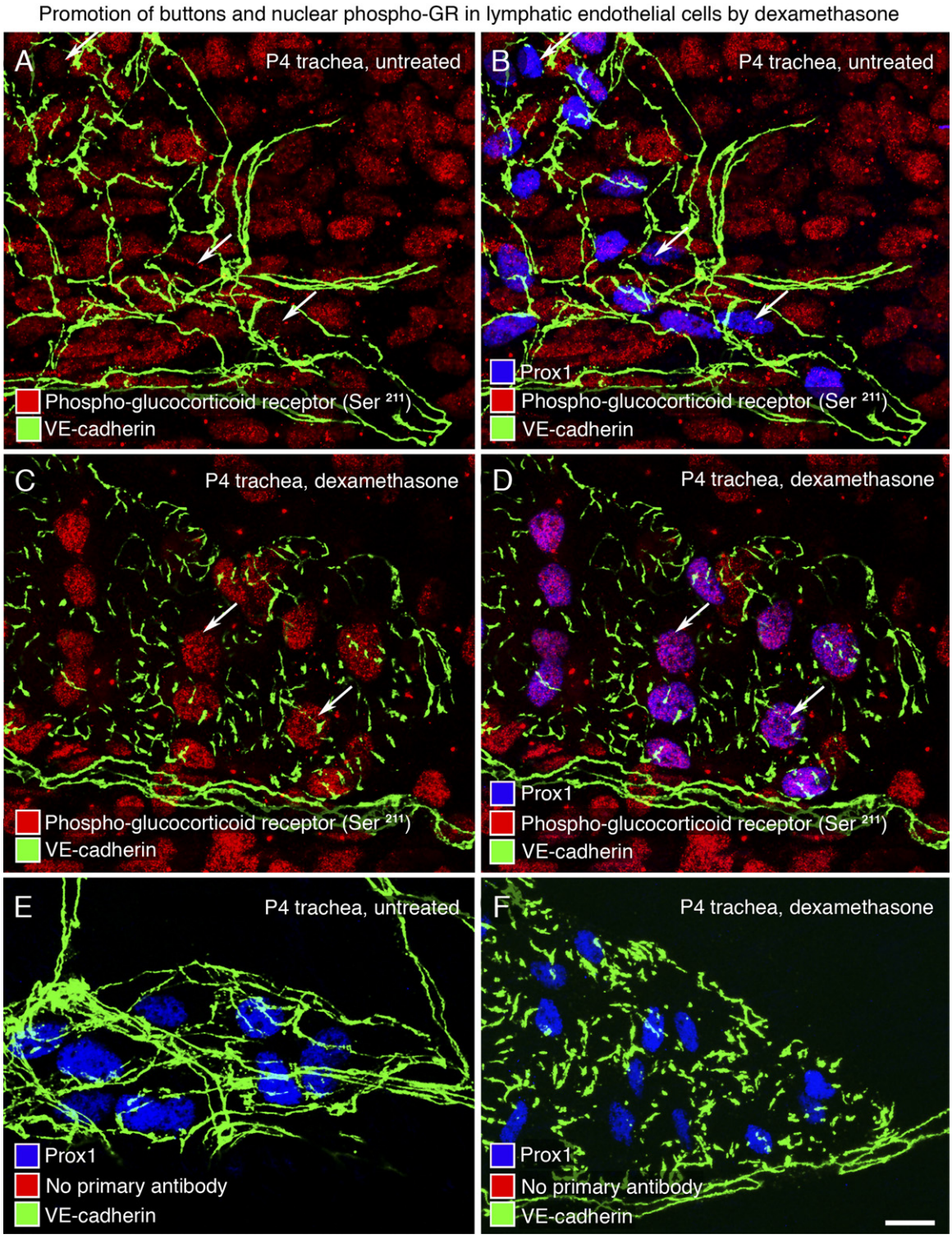

Figure 7. GR activation in lymphatics by dexamethasone at P4. **A–F:** Confocal images of lymphatics in tracheal whole mounts of untreated P4 pups (**A**, **B**, and **E**) or littermates treated with dexamethasone from P0 to P4 (**C**, **D**, and **F**). Endothelial cell junctions stained for VE-cadherin (green), nuclear phospho-GR Ser211 (red), and nuclear Prox1 (blue). **A** and **B:** Nuclear phospho-GR Ser211 is expressed in almost every cell in untreated trachea but is weak in lymphatic endothelial cells marked by Prox1 (red, **arrows**). **C** and **D:** After dexamethasone, nuclear phospho-GR Ser211 staining in lymphatic endothelial cells is stronger and more widespread, as shown by colocalization with Prox1 in nuclei (**D:** purple, **arrows**). **E** and **F:** Negative control (primary antibody for phospho-GR Ser211 was omitted). Scale bar = 20 μm.

cided with a corresponding decrease in intermediate junctions, when few zippers were still present.

The transformation of zippers into buttons coincided with changes in the shape of lymphatic endothelial cells from spindle to oak leaf and in the distribution of LYVE-1 during development. At E16.5 and earlier, LYVE-1 was uniformly distributed in lymphatics. Most of the transformation into the adult pattern, in which LYVE-1 is concen-

trated at the flaps at openings between buttons,[20,22] occurred from P0 to P28. LYVE-1, which is thought to be involved in hyaluronan homeostasis,[49] is one of the earliest markers expressed in lymphatics[50] and becomes largely restricted to initial lymphatics during lymphatic maturation.[51,52] The involvement of LYVE-1 in lymphatic function is, however, still uncertain because LYVE-1–null mice lack any apparent lymphatic abnormalities.[53,54]

Despite their structural differences, the same junctional proteins found in newly formed buttons were already present in zippers before the buttons formed. In both buttons and zippers, VE-cadherin was present in adherens junctions, and occludin, claudin-5, ZO-1, junctional adhesion molecule-A, and endothelial cell–selective adhesion molecule were present in tight junctions.[20,21] This finding suggests that the stepwise recruitment of proteins is not necessary for transformation of zippers into buttons or vice versa. Instead, the presence of intermediate forms of junctions during development could reflect a process of junctional maturation involving the redistribution of junctional proteins in the cell membrane.

The forces involved in the transformation of zippers into buttons are unclear, but the coincidence with birth is an important clue, because of the need for efficient clearance of amniotic fluid from the lungs after the onset of breathing. The importance of lymphatics in this process is evident from genetically engineered mice, in which development of lung lymphatics is suppressed by lung-specific overexpression of VEGFR-3 ectodomains that trap VEGF-C and VEGF-D. These mice have impaired lung fluid clearance and diminished survival after birth.[37] Hydraulic forces have pronounced effects on blood vessel remodeling in development,[55] and lymph flow influences fluid and cell transport functions of the lymphatic endothelium.[56]

The observation that most Prox1-positive cells were interconnected by junctions at E12.5 deserves further study, because lung lymphatics may form from single endothelial cells that migrate into lung parenchyma instead of from sprouting from other lymphatics.[37] Lymphangiogenesis could play a more important role at this stage than migration of single lymphatic endothelial cells.

Changes in Lymphatic Endothelial Cell Junctions in Airway Inflammation and Resolution

After *M. pulmonis* infection, lymphatic sprouts are evident at 7 days. The endothelium of the new vessels has zippers instead of buttons. By 14 days, the existing lymphatics, identified by their location between cartilage rings, also have zippers where buttons are normally located.

The finding that zippers replaced buttons in lymphatics in sustained inflammation raises the possibility that junctional alterations contribute to impaired fluid clearance and mucosal edema. If so, the reversal by dexamethasone of the zipper-to-button conversion and restoration of the oak leaf shape of lymphatic endothelial cells could improve fluid clearance and contribute to the beneficial effects of the steroid.

Additional studies will be needed to ascertain that buttons, and the flaps and openings between them, are components of the primary valves and that junctional changes in inflamed lymphatic endothelial cells lead to impaired fluid entry and edema. Although quantitative studies that have taught so much about lymphatic function in sheep and dogs[57] are much more challenging in mice, technological advances are likely to make this possible.[23,58,59]

Like dexamethasone, inhibition of VEGFR-3 signaling by antibody mF4-31C1 stopped further lymphangiogenesis after *M. pulmonis* infection, but unlike steroid treatment, VEGFR-3 blockade did not promote button formation. Although VEGFR-3 signaling is necessary and sufficient for lymphangiogenesis after the infection,[29] it was not required for the conversion of buttons into zippers.

Dynamics of Cell Junctions

Intercellular junctions are not static structures but can change under physiological and pathological conditions. The present understanding of the development and maturation of cell junctions is based largely on studies of epithelial and vascular endothelial cells, in which the integrity and barrier function of the layer is maintained by the number and distribution of adherens and tight junctions. In both cell types, adherens junctions form first in development and may regulate the subsequent assembly of tight junctions to form the barrier.[60–62]

Junctional dynamics have been extensively studied in the intestinal epithelium, where changes occur normally for absorption and in disease.[63,64] The presence of paracellular openings in the airway epithelium allows fluid and cell movement from the tissue into the lumen without influencing the epithelial cell integrity.[65,66] Junctional changes have also been proposed for primary valves of initial lymphatics, to explain the opening and closing during maintenance of tissue fluid homeostasis.[12] However, evidence that the primary valves are flap-covered, junctionless openings flanked by buttons argues that fluid and cell entry can occur without junctional remodeling, because the openings are always present.[20]

Junctional changes in the endothelium of blood vessels are well-documented features of inflammation. Many inflammatory mediators cause plasma leakage by triggering the formation of intercellular gaps between endothelial cells of venules.[27,67,68] In addition to the reorganization of junctional proteins, phosphorylation of VE-cadherin can weaken intercellular adhesion without apparent junctional rearrangement, and changes in transmural driving force and modifications of the endothelial glycocalyx can also influence the amount of plasma leakage in inflammation.[61,69]

Actin filament dynamics contribute to the stability and barrier function of vascular endothelial cells.[61,70–73] A rearrangement of the junction-associated cortical actin cytoskeleton could also be involved in the reorganization of the junctional proteins and LYVE-1 in lymphatic endothelial cells. The colocalization of the actin-binding proteins β-catenin and ZO-1 at zippers and buttons fits with the close relationship of the cytoskeleton and junctional proteins and raises the possibility that actin rearrangements could regulate the interconversion of buttons and zippers.

Dexamethasone Promotion of Junctional Maturation in Postnatal Development

Buttons were more abundant in neonates at age P4 after dexamethasone treatment than in age-matched controls. The promotion of button formation by dexamethasone in neonatal lymphatics was in the absence of inflammation, consistent with a steroid action beyond that of simply reducing the inflammatory response. Dexamethasone can improve the barrier function of tight and adherens junctions in cultured cells through effects on β-catenin and VE-cadherin.[74,75] The presence of phosphorylated GR in the nucleus of most cells indicates a baseline level of GR signaling in neonatal airways. However, phospho-GR immunoreactivity was stronger in nuclei of lymphatic endothelial cells after dexamethasone, consistent with direct effects of the steroid on these cells. The coincidence of increased GR activation and promotion of button formation after dexamethasone suggests a link between the two. Studies of GRs and glucocorticoid-deficient mice have documented the important role of GR signaling in lung development.[76] Formal elucidation of the mechanism of action of dexamethasone on lymphatic cell junctions will require further study, but the effects are beneficial.

In conclusion, intercellular junctions of lymphatic endothelial cells are dynamic during development and sustained inflammation. When lymphatics form during development, only zippers are present. Buttons first appear in initial lymphatics around birth. The conversion of zippers into buttons appears to result from transformation of one junctional type into the other via the formation of intermediate junctional forms. The reverse occurs in sustained inflammation, in which both newly formed and existing lymphatics have zippers but no buttons. Treatment with dexamethasone can reverse the process and restore buttons in initial lymphatics. Dexamethasone can also promote button formation in lymphatics during the neonatal period in the absence of inflammation. The steroid increases phosphorylated GRs in nuclei of lymphatic endothelial cells and thus the effects of dexamethasone on lymphatics are likely to be at least partly direct. Together, the findings document the plasticity of intercellular junctions in lymphatics and the potential for pharmacological manipulation. The precisely timed remodeling of lymphatic junctions during prenatal and postnatal development provides a model for identifying factors that influence lymphatic barrier function and maturation. Drugs that promote the transformation of zippers into buttons have potential therapeutic significance for ameliorating mucosal edema in inflammatory conditions of the airways, lungs, and other organs.

Acknowledgments

We thank Mary Brown (University of Florida) for production of the stock of *M. pulmonis* organisms and Kristoffer Larsen and Barbara Sennino for helpful discussion.

References

1. Tammela T, Alitalo K: Lymphangiogenesis: molecular mechanisms and future promise. Cell 2010, 140:460–476
2. Schulte-Merker S, Sabine A, Petrova TV: Lymphatic vascular morphogenesis in development, physiology, and disease. J Cell Biol 2011, 193:607–618
3. Witte MH, Jones K, Wilting J, Dictor M, Selg M, McHale N, Gershenwald JE, Jackson DG: Structure function relationships in the lymphatic system and implications for cancer biology. Cancer Metastasis Rev 2006, 25:159–184
4. Randolph GJ, Angeli V, Swartz MA: Dendritic-cell trafficking to lymph nodes through lymphatic vessels. Nat Rev Immunol 2005, 5:617–628
5. Johnson LA, Jackson DG: Cell traffic and the lymphatic endothelium. Ann N Y Acad Sci 2008, 1131:119–133
6. Pullinger BD, Florey HW: Some observations on the structure and functions of lymphatics: their behavior in local edema. Br J Exp Pathol 1935, 16:49–61
7. Drinker CK: The functional significance of the lymphatic system: Harvey lecture: December 16, 1937. Bull N Y Acad Med 1938, 14: 231–251
8. Leak LV, Burke JF: Fine structure of the lymphatic capillary and the adjoining connective tissue area. Am J Anat 1966, 118:785–809
9. Leak LV: Electron microscopic observations on lymphatic capillaries and the structural components of the connective tissue-lymph interface. Microvasc Res 1970, 2:361–391
10. Schmid-Schönbein GW: Microlymphatics and lymph flow. Physiol Rev 1990, 70:987–1028
11. Trzewik J, Mallipattu SK, Artmann GM, Delano FA, Schmid-Schonbein GW: Evidence for a second valve system in lymphatics: endothelial microvalves. FASEB J 2001, 15:1711–1717
12. Schmid-Schönbein GW: The second valve system in lymphatics. Lymphat Res Biol 2003, 1:25–29; discussion 29–31
13. Zawieja DC: Contractile physiology of lymphatics. Lymphat Res Biol 2009, 7:87–96
14. Norrmen C, Ivanov KI, Cheng J, Zangger N, Delorenzi M, Jaquet M, Miura N, Puolakkainen P, Horsley V, Hu J, Augustin HG, Yla-Herttuala S, Alitalo K, Petrova TV: FOXC2 controls formation and maturation of lymphatic collecting vessels through cooperation with NFATc1. J Cell Biol 2009, 185:439–457
15. Bazigou E, Xie S, Chen C, Weston A, Miura N, Sorokin L, Adams R, Muro AF, Sheppard D, Makinen T: Integrin-alpha9 is required for fibronectin matrix assembly during lymphatic valve morphogenesis. Dev Cell 2009, 17:175–186
16. Kanady JD, Dellinger MT, Munger SJ, Witte MH, Simon AM: Connexin37 and Connexin43 deficiencies in mice disrupt lymphatic valve development and result in lymphatic disorders including lymphedema and chylothorax. Dev Biol 2011, 354:253–266
17. Zhou F, Chang Z, Zhang L, Hong YK, Shen B, Wang B, Zhang F, Lu G, Tvorogov D, Alitalo K, Hemmings BA, Yang Z, He Y: Akt/protein kinase B is required for lymphatic network formation, remodeling, and valve development. Am J Pathol 2010, 177:2124–2133
18. Davis MJ, Rahbar E, Gashev AA, Zawieja DC, Moore JE Jr: Determinants of valve gating in collecting lymphatic vessels from rat mesentery. Am J Physiol Heart Circ Physiol 2011, 301:H48–H60
19. Niessen K, Zhang G, Ridgway JB, Chen H, Kolumam G, Siebel CW, Yan M: The Notch1-Dll4 signaling pathway regulates mouse postnatal lymphatic development. Blood 2011, 118:1989–1997
20. Baluk P, Fuxe J, Hashizume H, Romano T, Lashnits E, Butz S, Vestweber D, Corada M, Molendini C, Dejana E, McDonald DM: Functionally specialized junctions between endothelial cells of lymphatic vessels. J Exp Med 2007, 204:2349–2362
21. Dejana E, Orsenigo F, Molendini C, Baluk P, McDonald DM: Organization and signaling of endothelial cell-to-cell junctions in various regions of the blood and lymphatic vascular trees. Cell Tissue Res 2009, 335:17–25
22. Pflicke H, Sixt M: Preformed portals facilitate dendritic cell entry into afferent lymphatic vessels. J Exp Med 2009, 206:2925–2935
23. Tal O, Lim HY, Gurevich I, Milo I, Shipony Z, Ng LG, Angeli V, Shakhar G: DC mobilization from the skin requires docking to immobilized CCL21 on lymphatic endothelium and intralymphatic crawling. J Exp Med 2011, 208:2141–2153
24. Howarth P, Wilson J, Bousquet J, Rak S, Pauwels R: Airway Remodeling. Edited by C Lenfant. New York, Marcel Dekker, 2001, pp 167–188
25. Wilson JW, Kotsimbos T: Airway vascular remodeling in asthma. Curr Allergy Asthma Rep 2003, 3:153–158
26. McDonald DM: Infections intensify neurogenic plasma extravasation in the airway mucosa. Am Rev Respir Dis 1992, 146:S40–S44

27. McDonald DM: Angiogenesis and remodeling of airway vasculature in chronic inflammation. Am J Respir Crit Care Med 2001, 164:S39–S45
28. Pullinger BD, Florey HW: Proliferation of lymphatics in inflammation. J Pathol Bacteriol 1937, 45:157–170
29. Baluk P, Tammela T, Ator E, Lyubynska N, Achen MG, Hicklin DJ, Jeltsch M, Petrova TV, Pytowski B, Stacker SA, Yla-Herttuala S, Jackson DG, Alitalo K, McDonald DM: Pathogenesis of persistent lymphatic vessel hyperplasia in chronic airway inflammation. J Clin Invest 2005, 115:247–257
30. Kajiya K, Detmar M: An important role of lymphatic vessels in the control of UVB-induced edema formation and inflammation. J Invest Dermatol 2006, 126:919–921
31. Alexander JS, Chaitanya GV, Grisham MB, Boktor M: Emerging roles of lymphatics in inflammatory bowel disease. Ann N Y Acad Sci 2010, 1207(Suppl 1):E75–E85
32. El-Chemaly S, Levine SJ, Moss J: Lymphatics in lung disease. Ann N Y Acad Sci 2008, 1131:195–202
33. Zhou Q, Wood R, Schwarz EM, Wang YJ, Xing L: Near-infrared lymphatic imaging demonstrates the dynamics of lymph flow and lymphangiogenesis during the acute versus chronic phases of arthritis in mice. Arthritis Rheum 2010, 62:1881–1889
34. Truong T, Altiok E, Yuen D, Ecoiffier T, Chen L: Novel characterization of lymphatic valve formation during corneal inflammation. PLoS One 2011, 6:e21918
35. Kholova I, Dragneva G, Cermakova P, Laidinen S, Kaskenpaa N, Hazes T, Cermakova E, Steiner I, Yla-Herttuala S: Lymphatic vasculature is increased in heart valves, ischaemic and inflamed hearts and in cholesterol-rich and calcified atherosclerotic lesions. Eur J Clin Invest 2011, 41:487–497
36. Oliver G, Alitalo K: The lymphatic vasculature: recent progress and paradigms. Annu Rev Cell Dev Biol 2005, 21:457–483
37. Kulkarni RM, Herman A, Ikegami M, Greenberg JM, Akeson AL: Lymphatic ontogeny and effect of hypoplasia in developing lung. Mech Dev 2011, 128:29–40
38. Bowden JJ, Schoeb TR, Lindsey JR, McDonald DM: Dexamethasone and oxytetracycline reverse the potentiation of neurogenic inflammation in airways of rats with Mycoplasma pulmonis infection. Am J Respir Crit Care Med 1994, 150:1391–1401
39. Yao LC, Baluk P, Feng J, McDonald DM: Steroid-resistant lymphatic remodeling in chronically inflamed mouse airways. Am J Pathol 2010, 176:1525–1541
40. Barnes PJ: Corticosteroid effects on cell signalling. Eur Respir J 2006, 27:413–426
41. Zhuang T, Zhang M, Zhang H, Dennery PA, Lin QS: Disrupted postnatal lung development in heme oxygenase-1 deficient mice. Respir Res 2010, 11:142
42. Wigle JT, Harvey N, Detmar M, Lagutina I, Grosveld G, Gunn MD, Jackson DG, Oliver G: An essential role for Prox1 in the induction of the lymphatic endothelial cell phenotype. EMBO J 2002, 21:1505–1513
43. Ni A, Lashnits E, Yao LC, Baluk P, McDonald DM: Rapid remodeling of airway vascular architecture at birth. Dev Dyn 2010, 239:2354–2366
44. Srinivasan RS, Dillard ME, Lagutin OV, Lin FJ, Tsai S, Tsai MJ, Samokhvalov IM, Oliver G: Lineage tracing demonstrates the venous origin of the mammalian lymphatic vasculature. Genes Dev 2007, 21:2422–2432
45. Que J, Choi M, Ziel JW, Klingensmith J, Hogan BL: Morphogenesis of the trachea and esophagus: current players and new roles for noggin and Bmps. Differentiation 2006, 74:422–437
46. Zöltzer H: Morphology and Physiology of Lymphatic Endothelial Cells, In: Encyclopedia of the Microvasculature, Biology and Pathology 2006, 83:535–544
47. Dejana E, Tournier-Lasserve E, Weinstein BM: The control of vascular integrity by endothelial cell junctions: molecular basis and pathological implications. Dev Cell 2009, 16:209–221
48. Ismaili N, Garabedian MJ: Modulation of glucocorticoid receptor function via phosphorylation. Ann N Y Acad Sci 2004, 1024:86–101
49. Jackson DG: Immunological functions of hyaluronan and its receptors in the lymphatics. Immunol Rev 2009, 230:216–231
50. Banerji S, Ni J, Wang SX, Clasper S, Su J, Tammi R, Jones M, Jackson DG: LYVE-1, a new homologue of the CD44 glycoprotein, is a lymph-specific receptor for hyaluronan. J Cell Biol 1999, 144:789–801
51. Makinen T, Adams RH, Bailey J, Lu Q, Ziemiecki A, Alitalo K, Klein R, Wilkinson GA: PDZ interaction site in ephrinB2 is required for the remodeling of lymphatic vasculature. Genes Dev 2005, 19:397–410
52. Tammela T, Saaristo A, Holopainen T, Lyytikka J, Kotronen A, Pitkonen M, Abo-Ramadan U, Yla-Herttuala S, Petrova TV, Alitalo K: Therapeutic differentiation and maturation of lymphatic vessels after lymph node dissection and transplantation. Nat Med 2007, 13:1458–1466
53. Gale NW, Prevo R, Espinosa J, Ferguson DJ, Dominguez MG, Yancopoulos GD, Thurston G, Jackson DG: Normal lymphatic development and function in mice deficient for the lymphatic hyaluronan receptor LYVE-1. Mol Cell Biol 2007, 27:595–604
54. Luong MX, Tam J, Lin Q, Hagendoorn J, Moore KJ, Padera TP, Seed B, Fukumura D, Kucherlapati R, Jain RK: Lack of lymphatic vessel phenotype in LYVE-1/CD44 double knockout mice. J Cell Physiol 2009, 219:430–437
55. Lucitti JL, Jones EA, Huang C, Chen J, Fraser SE, Dickinson ME: Vascular remodeling of the mouse yolk sac requires hemodynamic force. Development 2007, 134:3317–3326
56. Miteva DO, Rutkowski JM, Dixon JB, Kilarski W, Shields JD, Swartz MA: Transmural flow modulates cell and fluid transport functions of lymphatic endothelium. Circ Res 2010, 106:920–931
57. Staub NC: Pulmonary edema. Physiol Rev 1974, 54:678–811
58. Proulx ST, Luciani P, Derzsi S, Rinderknecht M, Mumprecht V, Leroux JC, Detmar M: Quantitative imaging of lymphatic function with liposomal indocyanine green. Cancer Res 2010, 70:7053–7062
59. Kwon S, Sevick-Muraca EM: Functional lymphatic imaging in tumor-bearing mice. J Immunol Methods 2010, 360:167–172
60. Bazzoni G, Dejana E: Endothelial cell-to-cell junctions: molecular organization and role in vascular homeostasis. Physiol Rev 2004, 84:869–901
61. Dejana E, Orsenigo F, Lampugnani MG: The role of adherens junctions and VE-cadherin in the control of vascular permeability. J Cell Sci 2008, 121:2115–2122
62. Komarova Y, Malik AB: Regulation of endothelial permeability via paracellular and transcellular transport pathways. Annu Rev Physiol 2010, 72:463–493
63. Turner JR: Intestinal mucosal barrier function in health and disease. Nat Rev Immunol 2009, 9:799–809
64. Madara JL, Pappenheimer JR: Structural basis for physiological regulation of paracellular pathways in intestinal epithelia. J Membr Biol 1987, 100:149–164
65. Erjefalt JS, Erjefalt I, Sundler F, Persson CG: Epithelial pathways for luminal entry of bulk plasma. Clin Exp Allergy 1995, 25:187–195
66. Greiff L, Andersson M, Erjefalt JS, Persson CG, Wollmer P: Airway microvascular extravasation and luminal entry of plasma. Clin Physiol Funct Imaging 2003, 23:301–306
67. Schoefl GI: Studies on inflammation, III: growing capillaries: their structure and permeability. Virchows Arch Pathol Anat Physiol Klin Med 1963, 337:97–141
68. McDonald DM: Endothelial gaps and permeability of venules in rat tracheas exposed to inflammatory stimuli. Am J Physiol 1994, 266: L61–L83
69. Curry FR, Adamson RH: Vascular permeability modulation at the cell, microvessel, or whole organ level: towards closing gaps in our knowledge. Cardiovasc Res 2010, 87:218–229
70. Mehta D, Malik AB: Signaling mechanisms regulating endothelial permeability. Physiol Rev 2006, 86:279–367
71. Vandenbroucke E, Mehta D, Minshall R, Malik AB: Regulation of endothelial junctional permeability. Ann N Y Acad Sci 2008, 1123: 134–145
72. Bogatcheva NV, Verin AD: The role of cytoskeleton in the regulation of vascular endothelial barrier function. Microvasc Res 2008, 76:202–207
73. Spindler V, Schlegel N, Waschke J: Role of GTPases in control of microvascular permeability. Cardiovasc Res 2010, 87:243–253
74. Blecharz KG, Drenckhahn D, Forster CY: Glucocorticoids increase VE-cadherin expression and cause cytoskeletal rearrangements in murine brain endothelial cEND cells. J Cereb Blood Flow Metab 2008, 28:1139–1149
75. Guan Y, Rubenstein NM, Failor KL, Woo PL, Firestone GL: Glucocorticoids control beta-catenin protein expression and localization through distinct pathways that can be uncoupled by disruption of signaling events required for tight junction formation in rat mammary epithelial tumor cells. Mol Endocrinol 2004, 18:214–227
76. Whitsett JA, Matsuzaki Y: Transcriptional regulation of perinatal lung maturation. Pediatr Clin North Am 2006, 53:873–887, viii